The fast nucleation/growth of Co3O4 nanowires onto cotton silk: Facile development of potentiometric uric acid biosensor

Munirah Albaqami, Shymaa Medany, Ayman Nafady, Mazhar Hussain Ibupoto, Magnus Willander, Aneela Tahira, Umair Aftab, Brigitte Vigolo, Zafar Hussain Ibupoto

The fast nucleation/growth of Co_3O_4 nanowires onto cotton silk: Facile development of potentiometric uric acid biosensor

Munirah D. Albaqami[a], Shymaa S Medany, Ayman Nafady[a*], Mazhar Hussain Ibupoto[f], Magnus Willander[g], Aneela Tahira[c], Umair Aftab[d], Brigitte Vigolo[e], Zafar Hussain Ibupoto[c*]

[a] Department of Chemistry, College of Science, King Saud University, P.O. Box 2455, Riyadh 11451, Saudi Arabia

[b] Department of Chemistry, Faculty of Science, Cairo University, Cairo, Egypt

[c]Dr. M.A Kazi Institute of Chemistry University of Sindh Jamshoro, 76080, Sindh Pakistan

[d]Mehran University of Engineering and Technology, 7680 Jamshoro, Sindh Pakistan

[e]Université de Lorraine, CNRS, IJL, F-54000 Nancy, France

[f]Department of Zoology, Shah Abdul Latif University Khairpur Mirs

[g]Department of Science and Technology, Campus Norrköping, Linköping University, SE-60174 Norrköping, Sweden

Corresponding authors: Ayman Nafady, Zafar Hussian Ibupoto, PhD*,

Email address: anafady@ksu.edu.sa (AN); zaffar.ibhupoto@usindh.edu.pk

Abstract

In this study, we have used cotton silk as a source of abundant hydroxyl groups for the fast nucleation/growth kinetics of cobalt oxide (Co_3O_4) nanowires by hydrothermal method. The crystal planes of Co_3O_4 nanowires were well matched with the cubic phase. The as-synthesized Co_3O_4 nanowires were mainly containing the cobalt and oxygen elements, found to be highly sensitive towards uric acid in 0.01 M phosphate buffer solution of pH 7.4. Importantly, Co_3O_4 nanowires exhibited a large surface area which was heavily capitalized during the immobilization of uricase enzyme via physical adsorption method. The potentiometric response of uricase immobilized Co_3O_4 nanowires was measured for uric acid (UA) against the silver-silver chloride (Ag/AgCl) reference electrode. The newly fabricated uric acid biosensor possessed the lowest limit of detection of 1.0 ± 0.2nM with a wide linear range of 5 nM to 10 mM and a sensitivity of 30.6 $mVdec^{-1}$. Additionally, several related parameters of developed uric acid biosensor were investigated such as repeatability, reproducibility, storage stability, selectivity, and dynamic response time with satisfactory. The superior performance of Co_3O_4 nanowires was verified by fast charge transfer kinetics as confirmed by electrochemical impedance spectroscopy. A successful practicality of uric acid biosensor was evaluated by the recovery method. The observed performance of uricase immobilized Co_3O_4 nanowires revealed that it could be considered as a promising and an alternative tool for the detection of uric acid in both vitro and vivo conditions. Also, the use of cotton silk as a source of abundant hydroxyl groups may be considered for the remarkably fast nucleation/growth of other metal oxide nanostructures, thereby facilitating the fabrication of functional electrochemical devices such as batteries, water splitting and supercapacitors.

Keywords: Cotton silk, abundant hydroxyl groups, Co_3O_4 nanowires, uric acid biosensor

1. Introduction

Potentiometric method is a versatile electroanalytical approach to quantify the amount of small ions like H^+, K^+, F^- etc in the solution [1]. Potentiometric method does not involve the current bias like other electrochemical methods including chronoamperometry, differential pulse voltammetry and cyclic voltammetry. This highlights the superiority of potentiometric method and enables it

for operation in biological matrix without the damage. Potentiometric technique is very swift in the response and very simple and it does not require skilled person, therefore it can be used for the monitoring of uric acid at the on spot field [2-6]. Several potentiometric analysis are carried out annually via the use of classical membrane based ion selective electrodes. Today in the field of medical diagnosis and disease treatment, there is an immediate need to design and develop highly functional devices for the identification, detection and quantification of small biomolecules which play an important role in our body. The proposed devices should be fast in response, facile, sensitive, selective and highly accurate during the diagnosis of various diseases.

Uric acid (UA) is an antioxidant and present in urine or serum. UA is excreted by the kidney and resulted from the metabolism of purine nucleotide and its derivatives as end product and it causes many biological changes in our body [7,8]. The high concentrations of UA in fluids of our body [9] linked to many diseases including gout [10], hyperuricemia, Lesch-Nyhansyndrome [11], kidney and cardiovascular complications [7]. These medical issues confirms that the regular monitoring of UA is very essential, therefore various analytical methods are used to determine the UA such as high performance liquid chromatography (HPLC) [12], spectrophotometry [13], chemiluminescence and enzyme based biosensors [14, 15]. The UA biosensors are receiving more attention due to their numerous advantages such as simplicity, cost effectiveness, high sensitivity and excellent selectivity [16, 17, 18]. The uricase oxidase accelerates the oxidation of UA and transform it into allantoin. The high sensitivity and selectivity of uricase oxidase has revealed an excellent indicator for the development of efficient UA biosensor [19]. The first strategy follows for the transforming the biochemical reaction to electrical signal during the enzyme based amperometric biosensors for the quantification of redox species. The second strategy uses the electron transfer mediators between the active sites of enzymes and the electrode [20, 21]. However, the enzyme based approach has shown limited effectiveness, slow electrode kinetics and high over potential which ultimately impair the charge transfer and raises the issue of interference from other easily oxidizing substances. Also, the leach out of the soluble mediators from the electrode surface is unavoidable.

These major challenges in the development of UA biosensors are identified [22]. The use of efficient transducer is the pre-requirement for the development of UA biosensors which can easily overcome these limitations. Therefore, the synthesis of new functional transducers based on the nanostructured materials are appreciated by the scientific community in the field of material and

medical sciences. The use of nanostructured transducers enables the production of strong electrical signal due to their fast electron communication, and high surface area, therefore it can act as an excellent host material for the loading of enzymes. The outperform functionality of nanostructured materials is related to their high surface to volume ratio and rapid electron transfer activity [23]. The high performance of nanostructured materials is mainly governed by the size, chemical composition, specific surface area, catalytic activity and morphology [24].

A wide range of nanostructured materials like noble metal and metal oxides have been prepared and used for the sensing applications as a transducer is the main component of sensing devices [25-39]. The cobalt oxide (Co_3O_4) has superior advantages including high biocompatibility, narrow band gap material, excellent stability, low cost and produced from the earth abundant materials. These features of Co_3O_4 are largely studied for the electrochemical applications like sensors, supercapacitors and batteries [30, 41-46]. Therefore it is also well studied material for biomedical applications [40]. Also, Co_3O_4 exhibits significant stability and selectivity which are preferably and intensively studied for the sensing applications [47]. For improving the performance of Co_3O_4, various composite systems have been developed and used for the wide range of sensing applications [48-58]. Most of these composite systems involve multistep synthesis and they possess a complex structure. This is the reason why new and simple strategies are required for the synthesis of facile Co_3O_4 nanostructures with superior or equal performance to these reported composite based on Co_3O_4 materials. Still, the performance of Co_3O_4 is limited for electrochemical applications due to poor electrical conductivity, few catalytic sites and self-aggregation in the aqueous solution. Therefore, more attention is needed to synthesize Co_3O_4 nanostructures with improved electrical conductivity, high density of catalytic sites and well-dispersion in aqueous solution. For this purpose, we used a natural abundant source of hydroxyl groups from cotton silk which swiftly accelerated the nucleation rate of well oriented Co_3O_4 nanowires. The calcination of cotton silk provides abundant source of carbon in the chemical composition of Co_3O_4 nanostructures which can easily improve the dispersion of Co_3O_4 in aqueous solution. This can further enhance the electrochemical performance of Co_3O_4 nanostructures. Conclusively, cotton silk provides two aspects of improvement for Co_3O_4 including well controlled morphology and the dispersion. Therefore, the present study has overcome the main limitations of Co_3O_4 during electrochemical process and increased the performance of nanostructured Co_3O_4 towards the development of potentiometric uric acid biosensor.

In this study, we employed a high surface area and abundant hydroxyl groups for the fast nucleation of Co_3O_4 nanowires using two step approach. The nanostructures of Co_3O_4 were characterized by scanning electron microscopy (SEM), energy dispersive spectroscopy (EDS) and X-ray diffraction (XRD) and they were functionalized with uricase oxidase enzyme through electrostatic attraction. Then, the uricase immobilized nanostructured Co_3O_4 was used for the potentiometric determination of (UA) in the phosphate buffer solution of pH 7.4. The performance evaluation of UA biosensor was evaluated in terms of stability, selectivity, linear range, reproducibility and response time. The obtained results confirm that the proposed material could be used as an alternative transducer for the development of practical sensing devices.

2. Experimental details

2.1. Chemical reagents

The uricase oxidase enzyme of activity (E.C. 1.7.3.3), 25 units/1.5 mg received from Arthrobacter gloiformis, β-D-glucose (99.5%), uric acid (99.8%), 25% gultaradehyde, ascorbic acid, dopamine, urea, ethanol, cobalt chloride hexahydrate, potassium chloride, sodium, chloride, sodium biphosphate (Na_2HPO_4), sodium hydroxide, hydro chloric acid, and potassium dihydrogen phosphate (KH_2PO_4) were purchased from Sigma Aldrich Karachi Pakistan. All the chemicals were of analytical grade and used without further purification. A 0.01 M phosphate buffer solution of pH 7.4 prepared by mixing 0.01 M sodium chloride, 0.02 M potassium chloride, 0.001 M KH_2PO_4,and 0.005 M Na_2HPO_4 into deionized water. The deionized was used as a main solvent media. The cotton silk was obtained from local market of Hyderabad Sindh Pakistan.

2.2. Preparation of Co_3O_4 nanowires on cotton silk by hydrothermal process

The fabrication of Co_3O_4 nanostructures onto the cotton silk was done through hydrothermal process followed by combustion reaction. Prior to the hydrothermal process, the cotton silk was washed gently with the deionized water and ethanol. Then a wet piece of cotton silk was dipped into 0.1 M solution of cobalt chloride hexahydrate and urea until it was settled at the bottom of beaker. Afterwards, the cobalt precursors containing a wet piece of cotton silk was covered tightly with aluminum sheet and put into the preheated electric oven at 95 ^oC for 4 h. Then, a pink layer was coated on the cotton silk and washed several times with the deionized water and left to dry for

overnight. Then, the combustion reaction was carried on the pink product deposited on the cotton silk for 4 h at 450 ^{o}C in air. A shiny blackish product was successfully prepared. The synthesis of pristine Co_3O_4 nanostructures was carried out by the same method without the use of cotton silk.

The morphology and composition of as obtained Co_3O_4 nanostructures was studied through the use of low resolution scanning electron microscopy operated at 3 kV. The elemental analysis of Co_3O_4 nanostructures was done on the energy dispersive spectroscopy equipped with SEM. The powder X-ray diffraction was used to identify the crystal planes and purity of as prepared Co_3O_4 nanostructures. The XRD measurements were done using x rays from CuKα radiation ($\lambda = 1.54050$ Å), at 45 mA, and 45 kV. The potentiometric experiments were performed on the pH meter METTLER TOLEDO and the dynamic response was measured through the potentiostat supplied from Netherland. The charge transfer evaluation was carried out via electrochemical impedance spectroscopy (EIS) using the experimental conditions of 50 KHz to 10 Hz, sinusoidal potential of 5 mV and zero supplied potential at room temperature, 0.1 mM uric acid prepared in 0.01 M phosphate buffer solution of pH 7.4. The Z-view software was used to simulate the experimental data with fitted an equivalent circuit for enabling the authenticity of measured data.

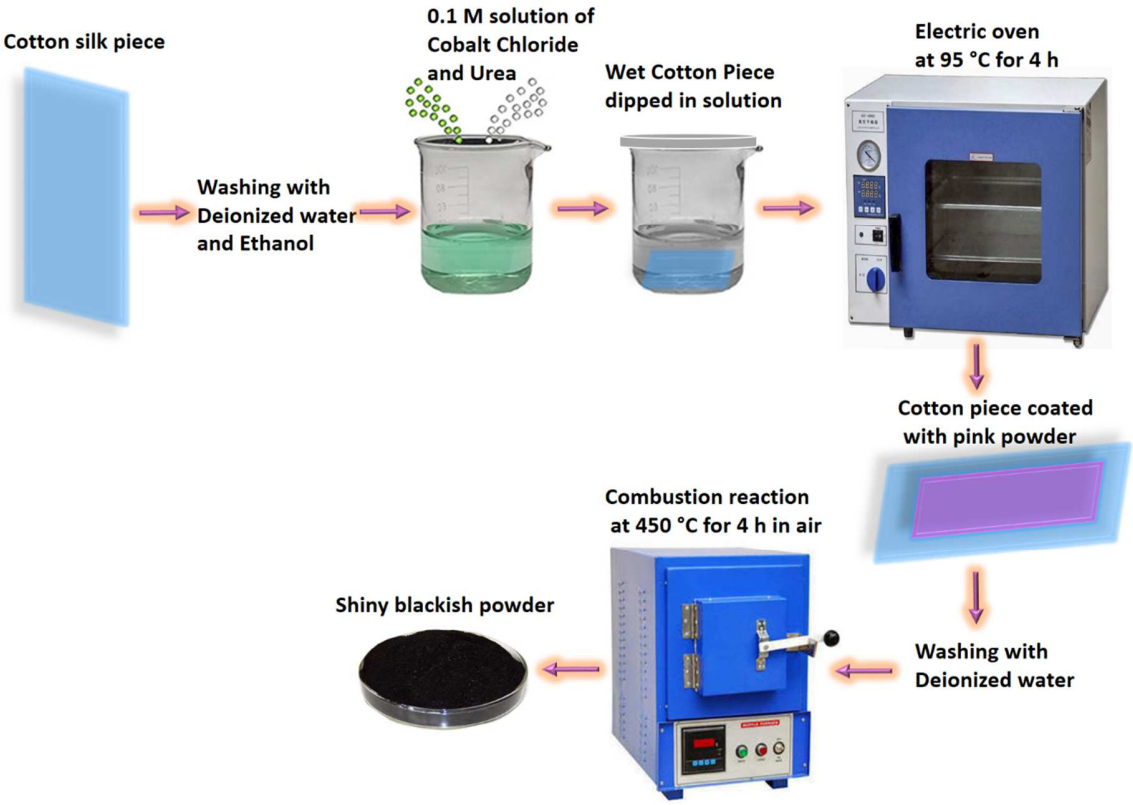

Scheme 1: Synthesis process of the prepared Co_3O_4 nanostructures.

2.3. Modification of uricase immobilized Co_3O_4 nanostructures onto the glassy carbon electrode.

The cleaning of glassy carbon electrode was done according to our published work [59]. Briefly cleaning of glassy carbon electrode was done with alumina paste of 5 µm and silica paper, then it was washed several times with deionized water and dried with the blow of air. The potentiometric response of pristine and cotton silk deposited Co_3O_4 nanostructures was measured in 0.01M phosphate buffer solution of pH 7.4. The immobilization of uricase onto 10 mg of Co_3O_4 nanostructures was done in the phosphate buffer solution containing 10 mg of uricase and 100 µliter of 1% glutaraldehyde. The soaking of Co_3O_4 nanostructures with uricase enzyme solution was performed for 30 min in order to get a full coverage of enzyme molecules with the Co_3O_4 nanostructures. Then, 10 µl of uricase enzyme immobilized Co_3O_4 nanostructures with a

loading mass of 0.2 mg were deposited on the cleaned glassy carbon electrode via drop casting process. Then, the modified electrode was dried at room temperature followed by overnight soaking into the phosphate buffer solution of pH 7.4 due to get a stable output potential response. Then, the soaked electrode was dried at atmospheric conditions and ready to measure the sensing of uric acid oxidation. The glassy carbon electrode of 3 mm area was sued and thickness of sensing layer could be around 50 nm.

The modified electrode was labelled as working electrode and its output potential was measured against the reference silver-silver chloride (Ag/AgCl) electrode filled with 3M KCl. A two electrode set up was used as an electrochemical cell containing the specific concentration of uric acid prepared in the 0.01 M phosphate buffer solution of pH 7.4. For stock solution, we first heated the uric acid (UA) in 1 M NaOH aqueous solution at 75 ºC for 3 h, then we made the stock solution of 15 mM in phosphate buffer solution by adjusting the pH around 7.4 using concentrate hydrochloric acid solution. Afterwards, we used dilution equation for the preparation of low concentrations of UA. All the studied were done at room temperature other than the effect of temperature on the potentiometric signal.

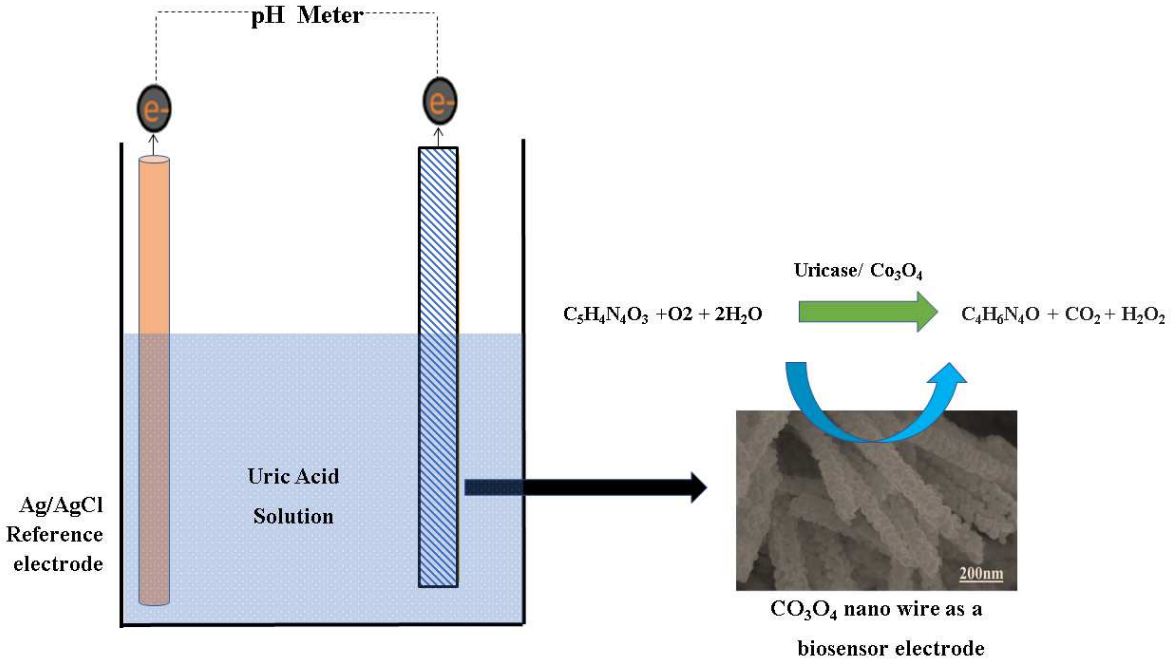

Scheme 2: Sensing mechanism of UA on uricase immobilized onto Co_3O_4 nanostructures

3. Results and discussion

3.1. The crystalline, morphology and composition studies of Co_3O_4 nanostructures

The typical diffraction patterns of pristine and cotton silk deposited Co_3O_4 nanostructures are shown in Figure 1a-b. The crystal planes of pristine Co_3O_4 nanostructures indicates the pure cubic phase and they are fully supported by the reference card no :00-009-0418. However, the cotton silk deposited Co_3O_4 nanostructures have shown similar diffraction patterns but slightly shifted towards higher angle as shown in Figure 1b. The crystal planes of cotton silk deposited Co_3O_4 nanostructures are also in good agreement with above reference card. The XRD study has verified that no any other impurity of carbon from cotton was found, suggesting that cotton can be used as a high surface substrate to deposit large surface area metal oxide nanostructures.

The morphology of as prepared Co_3O_4 nanostructures was investigated by SEM analysis as shown in Figure 2. The pristine Co_3O_4 nanostructures possess a platelet like morphology consisting a self-assembly of nanoparticles as shown in Figures 2a-b. The length of Co_3O_4 platelets is in microns and the nanoparticles are in size of 100 nm. The use of cotton silk as a high surface area substrate has evolved the nanowire like Co_3O_4 nanostructures. Also, these nanowires of Co_3O_4 are few microns in length with average diameter of 100-200 nm. The nanowires are evolved from the self-assembly of nanoparticles. The evolution of nanowires might be assigned to plenty of hydroxyl groups present in the cotton silk which accelerated the growth kinetics through swift nucleation. Further to add, the presence of hydroxyl groups on the substrate surface could be useful to bind the metal ions which act a nucleation units for the development of metal hydroxide crystals, thereby not only the growth kinetics is enhanced, but the evolution of morphology could not be excluded.

The composition of as prepared Co_3O_4 nanostructures was also analyzed using EDS analysis as shown in Figures 3a-b. The pristine Co_3O_4 nanostructures and cotton silk deposited Co_3O_4 nanowires has shown only cobalt and oxygen as the main elements as shown in Figures 3a-b. The point of notice is the relative amount of oxygen is low in the Co_3O_4 nanowires indicating more oxygen vacancies in the sample as shown in Figure 3b.

3.2. Potentiometric response of uricase immobilized Co_3O_4 nanostructures towards sensing of uric acid

The use of standard two electrode cell up could be described as under:

Co_3O_4| Co^{+3}/ Co^{+2} PBS sol||Ag/AgCl PBS sol |Ag

The output potential of the electrochemical cell depends on the ionic charges present in the electrolytic solution and the response of output potential could be related to the amount of charged species in the testing solution through the calibration fitting. The Co_3O_4 nanostructures were immobilized with uricase enzyme, then tested for the detection of UA. It is well established that uricase enzymes specifically oxidize uric acid, consequently the generation of different charged species is always expected. However, the role of Co_3O_4 nanowires in this configuration was not only to provide high surface to volume ratio for the heavy loading of uricase enzyme, but its role of co-catalyst and promoter for uricase enzyme is obvious through the strong output potential signal during the oxidation of UA. The potentiometric studies were initiated with the soaked modified electrode in the 0.01 M phosphate buffer solution of pH 7.4 and a stable output potential was noticed, however an addition of 1 nM uric acid resulted an unstable signal but further addition of 5 nM uric acid has shown a stable and repeatable signal. Therefore, the calibration curve was made from 5 nM to 10 mM as shown in Figure 4c. Figure 4a shows the potentiometric response of uricase immobilized pristine Co_3O_4 platelets indicating a poor output signal, and analytical performance. The narrow range of uric acid from 0.005-1mM and regression coefficient of 0.95 doubts on the accuracy and precision of uric acid biosensor based on the uricase immobilized pristine Co_3O_4 nanostructures. The poor performance of pristine Co_3O_4 nanostructures is associated to the improper and weak immobilization of uricase enzyme due to randomly oriented morphology of Co_3O_4 nanostructures. The Co_3O_4 nanowires without immobilization were also tested for the detection of UA as shown in Figure 4b. It is obvious that the Co_3O_4 nanowires have relatively some increased value of output potential compare to the pristine Co_3O_4 platelets, indicating that well oriented morphology has better compatibility for the interaction of uric acid molecules and contribution towards the fast electron communication. However, the performance of Co_3O_4 nanowires without the loading of uricase enzyme is still weak, therefore we aimed to use the immobilization of uricase enzyme onto the surface of Co_3O_4 nanowires via physical adsorption for the development of sensitive and selective potentiometric uric acid biosensor. For this reason, the activity of Co_3O_4 nanowires is superior due to high surface to volume ratio for the excellent immobilization of uricase enzyme as shown in Figure 4b. The potentiometric response of proposed

Co_3O_4 nanowires is highly sensitive to a to be analyzed substrate compound and throughout the study modified electrode has followed the Nernst's equation

$$E = E^0 - 0.05916\ V/\ n \log {}^{[Reduced]} / {}_{[Oxidized]}$$

The generation of output potential on the surface of uricaze immobilized Co_3O_4 nanowires could be attributed to the co-catalytic and promoter role of Co_3O_4 nanowires towards the oxidation of uric acid.

For the measurement of uric acid concentration by the proposed uric acid biosensor, the biosensor electrode should be associated with an excellent range[60]. The output potential of modified electrode was evaluated in various uric acid concentrations ranging from 5 nM to 10 mM prepared in the phosphate buffer solution of pH 7.4 as shown in Figure 4b. The modified electrode demonstrated an excellent analytical features such as regression coefficient of 0.99, wide linear and low limit of detection of 1.0 ± 2 nM. The potentiometric curve exhibited an excellent correlation with log of uric acid concentration as shown in Figure 4b. The limit of detection and limit of quantification of 1.0 ± 0.2 nM were calculated according to the published work[61]. The modified electrode has shown a quick response time and a sensitivity of 30.5 $mVdec^{-1}$. From Figure 4c, the Nernst factor was observed about 30.5 mV/decade as uric acid is divalent molecules as shown in scheme 2. Therefore, Nernst factor estimated is (61/2) mV/decade that equals to 30.5 mV/decade (±1-3 mV).

The linear range, response time and sensitivity of uricase immobilized Co_3O_4 nanowires are superior than the pristine uricase immobilized Co_3O_4 platelets due to the well oriented morphology, high surface to volume ratio, favorable and highly compatible surface for high loading of uricase enzyme molecules. It has been found that the one-dimensional nanowire is associated with fast charge transport, and it is always expected that well controlled Co_3O_4 nanowires are highly needed for the development of electrochemical devices. Moreover, the Co_3O_4 offers unique p-type character for frequent interaction towards three oxygenated atoms of uric acid which ultimately may foster the reaction kinetics on the surface of Co_3O_4 nanowires, therefore we observed an outstanding potentiometric performance. Furthermore, the sign of output potential during the potentiometric determination of uric acid could be attributed to equilibrium established between the electrode and the analyte. UA is easily oxidzable compound, therefore it might oxidize differently on various electrodes. Also, uric acid is an acid. This means that it could work as a

dopant etc. Hence, we should not be surprised about the sign of the output potential either it can be positive or negative.

A fast and sensitive electroanalytical method is always needed to monitor the bioactive compounds from the biological samples for ensuring the rapid biomedical diagnosis and treatment. For this purpose, the response time of modified electrode was monitored in 1 mM uric acid as shown in Figure 5. The response time describes the kinetics and sensitivity of modified electrode towards sensing of specific concentration of uric acid and the proposed uric acid biosensor based on uricase immobilized Co_3O_4 nanowires exhibited a fast response time of less than 1 s. Additionally, response time is also showing that the modified electrode is stable and did not change the output potential with time as shown in Figure 5. The repetitive use of electrode is another way to confirm the stability of sensing layer onto the glassy carbon electrode as well as number of times of use of modified electrode. The use of the same modified electrode for the several times is worthy to investigate, therefore we studied the repeatability of modified electrode for three times at alternative days in the same dynamic range of uric acid concentration. We found that the presented electrode is highly repeatable and did not bring any significant change in the sensitivity, linear range and limit of detection as shown in Figure 6, confirming high stability and an excellent repeatability response of sensing layer onto glassy carbon electrode. The repeatability experiment has verified an excellent performance of modified electrode due to firm adhesion and high biocompatibility of uricase enzyme with the surface of well oriented Co_3O_4 nanowires. The inter electrode response of modified electrode is very essential to study as it could confirm the accuracy and precision of modification process. The quantitative response of different modified electrodes prepared under the same conditions through inter-electrode study is shows the figure of merit of modified electrode in terms of reliable analytical performance.

Therefore, we studied the reproducibility of seven independently proposed Co_3O_4 nanowires in 0.1 mM uric acid testing solution as shown in Figure 7.

The potentiometric response indicates that the response of inter-electrode systems is very reproducible with standard deviation of less than 5 % revealing an excellent analytic performance. Thus, the Co_3O_4 nanowires could be considered as a potential and alternative material to immobilize uricase at the large scale for the practical monitoring of uric acid. The selectivity is

one of the main parameters to evaluate the performance of uric acid biosensor as some of the interfering substances such as ascorbic acid, dopamine and glucose are influencing on the performance of biosensor. Therefore, we studied the effect of 0.1 mM concentration of these substances in the presence of 0.01 mM uric acid on the output potential of uric acid biosensor using sequential addition method as shown in Figure 8.

It is clear from this study, that Co_3O_4 nanowires functionalized with uricase enzyme has high selectivity towards uric acid sensing, thus modified electrode may of be of great interest under vivo conditions. This study has confirmed that the negligible interference during the uric acid detection was observed and no significant change in the output potential was noticed when the interfering substances were added in the uric acid solution. Despite the generation of charges after the addition of these interfering substances, which might be counterbalanced by the ionic strength of phosphate buffer solution, thus these charges have shown a negligible impact in producing the output potential as shown in Figure 8. The outstanding selectivity of presented uric acid biosensor could be further contributed from the selective nature of uricase enzyme for the uric acid and also less likely compatibility of Co_3O_4 nanowires for the interfering substances. The pH of analytic solution can have influence on the activity of sensing layer of the electrode in terms of Co_3O_4 material stability and the decreasing the effectiveness of urease enzyme at certain pH values. Therefore, the response of uricase modified electrode can be affected by changing the pH of electrolyte, therefore, we studied the effect of different pH values in 0.5mM uric acid on the biosensor signal as shown in Figure 9a. This study resulted the optimum pH around 7.0 for the modified electrode and it showed a maximum output potential. Also, it is reported that the activity of uricase is higher in the pH range of 8.5 to 9.2 [60]. We have already reported a pH sensor based on Co_3O_4[62]. We studied the effect of pH on the EMF of only Co_3O_4 nanowires for the illustration of pH sensor, however the reported work suggests that the pH has significant effect on the stability of Co_3O_4[60], and for this purpose we studied the effect of pH on the performance of uric acid biosensor based on Co_3O_4 nanowires. Thus, it was observed as instable under highly alkaline and acidic conditions due to dissolution and etching effects as shown in Figure 9a. Also, there is possibility at high alkaline conditions the involvement of hydroxyl groups with uricase enzyme that might alter the kinetics of UA oxidation, consequently performance of proposed biosensor could be decreased. Keeping in view these limitations of sensing layer and the physiological

conditions of uric acid detection from the real samples, hence we studied the biosensing evaluation parameters of our proposed Co_3O_4 nanowires based uric acid biosensor around pH 7.4[53,58].

The pH 7.4 is close to that of pH of human body fluids, therefore all the studies were done at this pH except pH study. For the biosensors based on the biosensitive membranes, the influence of environmental temperature is a big challenge due to denaturation of biosensitive membranes like antibodies, enzymes, nuclease etc. Thus, to confirm the storage conditions and to enhance the lifetime of biosensor we evaluated the performance of uric acid biosensor at various temperatures as shown in Figure 9b. This suggests that the optimum temperature of presented uric acid biosensor is around 40 ^oC, indicating that biosensor has maximum output potential generation at this temperature. Additionally at higher temperature, the activity of sensing layer was decreased to the denaturation of uricase enzyme. Therefore, we measured and observed the potentiometric response at 20 ^oC to prevent the denaturation of uricase enzyme and to avoid the evaporation of testing solution. An acceptable lifetime of proposed uric acid biosensor is highly needed for the performance evaluation. The storage period of uricase immobilized nanowires obtained with cotton silk was also studied by monitoring the linear range, limit of detection and sensitivity as given in Table 1. It is obvious that the proposed modified electrode can be used for the time of more than 6 weeks, if the storage conditions are maintained. This study suggests that the enzyme activity remains almost same even after the use of 6 weeks due to possible role of high biocompatibility of Co_3O_4 nanowires. We stored the modified electrode at 4 ^oC in the refrigerator when not in use.

The activity uricase enzyme immobilized Co_3O_4 nanowires was also compared with the recently reported non-enzymatic uric acid sensors either based on Co_3O_4 or other materials. It is obvious that the presented approach has superior performance than many of the published results in terms of wide linear range, limit of detection and the most importantly the simple and easy approach for the synthesis of nanostructured materials. The low cost and environment friendly synthesis aspects of Co_3O_4 nanowires strengthened the scalable fabrication of potentiometric uric acid biosensors[63-65].

Figure 10 shows the typical Nyquist plots for the demonstration of charge transfer during potentiometric measurement of uric acid and inset is describing the fitted equivalent circuit with well-defined elements. The Co_3O_4 nanowires experienced a faster charge transfer as observed form

the small arc of Nyquist plot suggesting that nanowires have better electrical communication channels that the platelet like structure of Co_3O_4. However, after the immobilization of uricase enzyme, we see a slight increase in impedance due to insulating features of uricase enzyme and glutaraldehyde and these observations are in full agreement with the published works [66]. Furthermore, the estimated value of impedance for the Co_3O_4 nanowires is lower than the platelet like structure of the Co_3O_4 as given in Table 2 and verifying the above claims based on the faster charge transfer of the Co_3O_4 nanowires. The analytical performance of uricase immobilized nanowires obtained with cotton silk was also evaluated through % recovery method as given in Table 3. The obtained % recovery results were found compatible and suggests that the proposed structure of uric acid could be applied for the practical applications of uric acid determination. The comparative analysis of presented results with the recently published results on the enzymatic approach is given in Table 4 [67-72]. The obtained results of Co_3O_4 nanowires are superior in terms of wide linear range, limit of detection and fast response time, revealing the role of cotton silk in driving the co-catalytic role of Co_3O_4 nanowires towards uricase enzyme for the oxidation of uric acid.

4. Conclusions

An abundant hydroxyl groups of cotton silk have been utilized for the fast nucleation/growth kinetics of well oriented Co_3O_4 nanowires via hydrothermal method. The composition of Co_3O_4 nanowires as confirmed by XRD and SEM images contained only cobalt and oxygen as the main elements. The prepared Co_3O_4 nanowires exhibited a large surface area which favored the high loading of uricase enzyme through physical adsorption. The strong binding of uricase with Co_3O_4 nanowires enabled the fabrication of sensitive and selective potentiometric uric acid biosensor in 0.01 M phosphate buffer solution of pH 7.4. A wide working linear range from 5 nM to 10 mM (UA) concentration and the lowest limit of detection of 1.0 ± 0.2nM of presented uric acid biosensor is reported. The important analytical parameters such as reproducibility, stability, response time and selectivity were found satisfactory. The recovery method was used to verify the practical aspect of fabricated biosensor and it was found satisfactory. The obtained performance suggests that the uric acid biosensor based on uricase immobilized Co_3O_4 nanowires could be used as a potential protocol for the determination of uric acid. The use of cotton silk as a source of

abundant hydroxyl groups for the fast nucleation of metal oxide nanostructures could be of great interest for the scientists and researchers for the desired applications.

Acknowledgements

We extend our sincere appreciation to the Researchers Supporting Project (RSP-2022/79) at King Saud University, Riyadh, Saudi Arabia.

Conflict of Interest statement

Authors declare no conflict of interest in this research work

5. References

1. E. Bakker, Potentiometric Sensors, Environmental Analysis by Electrochemical Sensors and Biosensors, Springer, 2014, pp. 193-238.

2. E. Lindner, B.D. Pendley, 2013, 762, 1-13.

3. E. Bakker, E. Pretsch, Modern potentiometry, *Ang. Chemie.Int.* Ed, 2007, 46, 5660-5668.

4. A. Düzgün, G.A. Zelada-Guillén, G.A. Crespo, S. Macho, J. Riu, F.X. Rius, *Ana. and bioanalytical Chem.*, 2011, 399, 171-181.

5. J. Ding, W. Qin, *Tr. in Ana. Chem,* 2020, 124, 115803.

6. E. Zdrachek, E. Bakker, Analytical chemistry, 2018, 91, 2-26.

7. K. Arora, M. Tomar, V. Gupta, *Bio. and Bioelec.,* 2011, 30, 333-336.

8. S. Jain, S. Verma, S.P. Singh, S.N. Sharma, *Bio. and Bioelec* 2019, 127, 135-141.

9. K.L. Rock, H. Kataoka, J.-J. Lai, *Nat. Rev. Rheum.*, 2013, 9, 13-23.

10. W. Nyhan, *J.of inher. Metab. diseas*, 1997, 20, 171-178.

11. D. Swinson, J. Snaith, J. Buckberry, M. Brickley, *Int. J. of Osteor.,* 2010, 20, 135-143.

12. D.L. Rocha, F.R. Rocha, *Micro. J.,* 2010, 94, 53-59.

13. D. Jin, M.-H. Seo, B.T. Huy, Q.-T. Pham, M.L. Conte, D. Thangadurai, Y.-I. Lee, *Bio. and Bioelec*, 2016, 77, 359-365.

14. Y. Zhang, H. Jin, X. Li, J. Zhao, X. Guo, J. Wang, Z. Guo, X. Zhang, Y. Tao, Y. Liu, *J. of Chrom. B*, 2016, 1026 , 67-74.

15. H. Dai, N. Wang, D. Wang, X. Zhang, H. Ma, M. Lin, *Micro. Acta*, 2016, 183, 3053-3059.

16. C. Hou, H. Liu, D. Zhang, C. Yang, M. Zhang, *J. of Allpy and Comp*., 2016, 666, 178-184.

17. J. Zhao, F. Mu, L. Qin, X. Jia, C. Yang, *Mate. Chem. and Phy.,* 2015, 166, 176-181.

18. G. Rocchitta, A. Spanu, S. Babudieri, G. Latte, G. Madeddu, G. Galleri, S. Nuvoli, P. Bagella, M.I. Demartis, V. Fiore, *Sensors,* 2016, 16, 780.

19. A. Vijayakumar, E. Csöregi, A. Heller, L. Gorton, *Analyt. Chimica.Acta,* 1996, 327, 223-234.

20. S. Dong, B. Wang, B. Liu, *Bio. and Bioelec*, 1992, 7 , 215-222.

21. P.E. Erden, E. Kılıç, *Talanta,* 2013, 107, 312-323.

22. H. Yao-Juan, D. Wen-Ji, C. Chang-Yun, *Chin. J. of Analyt. Chem.,* 2014, 42, 1240-1244.

23. B.T. Sneed, A.P. Young, D. Jalalpoor, M.C. Golden, S. Mao, Y. Jiang, Y. Wang, C.-K. Tsung, Acs Nano, 2014, 8, 7239-7250.

24. R.A. Soomro, O.P. Akyuz, R. Ozturk, Z.H. Ibupoto, *Sens. and Actuat. B: Chemical,* 2016, 233, 230-236.

25. H. Mei, W. Wu, B. Yu, H. Wu, S. Wang, Q. Xia, *Sens. and Actuat. B: Chemical,*, 2016, 223 , 68-75.

26. Q. Sheng, H. Mei, H. Wu, X. Zhang, S. Wang, *Sens. and Actuat. B: Chemical,*, 2015, 207, 51-58.

27. S. Poyraz, Z. Liu, Y. Liu, N. Lu, M.J. Kim, X. Zhang, *Sens. and Actuat. B: Chemical,*, 2014, 201, 65-74.

28. H. Wang, X. Bo, L. Guo, *Sens. and Actuat. B: Chemical,*, 2014, 192,181-187.

29. J.S. Chung, S.H. Hur, *Sens. and Actuat. B: Chemical,* 2016, 223, 76-82.

30. M. Chowdhury, F. Cummings, M. Kebede, V. Fester, *Electroanalysis,* 2017, 29, 578-586.

31. J. Xu, N. Xu, X. Zhang, P. Xu, B. Gao, X. Peng, S. Mooni, Y. Li, J. Fu, K. Huo, *Sens. and Actuat. B: Chemical,*, 2017, 244, 38-46.

32. M. Baghayeri, H. Veisi, M. Ghanei-Motlagh, *Sens. and Actuat. B: Chemical,* 2017, 249 , 321-330.

33. Y. Ni, J. Xu, Q. Liang, S. Shao, *Sens. and Actuat. B: Chemical,* 2017, 250, 491-498.

34. H. Wu, Y. Yu, W. Gao, A. Gao, A.M. Qasim, F. Zhang, J. Wang, K. Ding, G. Wu, P.K. Chu, *Sens. and Actuat. B: Chemical,* 2017, 251, 842-850.

35. R. Ghosh, J. Ghosh, R. Das, L.P. Mawlong, K.K. Paul, P. Giri, *J. of coll.and interface. science*, 2018, 532 , 464-473.

36. S. Wang, S. Zhang, M. Liu, H. Song, J. Gao, Y. Qian, *Sens. and Actuat. B: Chemical,* 2018, 254, 1101-1109.

37. L. Liu, Z. Wang, J. Yang, G. Liu, J. Li, L. Guo, S. Chen, Q. Guo, *Sens. and Actuat. B: Chemical,*, 2018, 258 , 920-928.

38. Y. Liu, A.P. Turner, M. Zhao, W.C. Mak, *Biosen. and Bioelect.,* 2018, 100 , 374-381.

39. L. Ding, M. Zhao, S. Fan, Y. Ma, J. Liang, X. Wang, Y. Song, S. Chen, *Sens. and Actuat. B: Chemical,*, 2016 , 235, 162-169.

40. B. Dalkiran, C. Kacar, P.E. Erden, E. Kilic, Sensors and Actuators B: Chemical, 2014, 200, 83-91.

41. Y. Haldorai, J.Y. Kim, A.E. Vilian, N.S. Heo, Y.S. Huh, Y.-K. Han, *Sens. and Actuat. B: Chemical,* 2016, 227, 92-99.

42. T. Zhou, P. Lu, Z. Zhang, Q. Wang, A. Umar, *Sens. and Actuat. B: Chemical,*, 2016, 235 , 457-465.

43. L. Li, C. Zhang, R. Zhang, X. Gao, S. He, M. Liu, X. Li, W. Chen, *Sens. and Actuat. B: Chemical,* 2017, 244, 664-672.

44. J.-W. Kim, S.J. Lee, P. Biswas, T.I. Lee, J.-M. Myoung, *App. Surf. Scien,* 2017, 406 , 192-198.

45. X. Qing, S. Liu, K. Huang, K. Lv, Y. Yang, Z. Lu, D. Fang, X. Liang, *Electro. Acta,* 2011, 56, 4985-4991.

46. S. Fan, M. Zhao, L. Ding, Y. Ma, J. Liang, X. Wang, Y. Song, S. Chen, *Sens. and Actuat. B: Chemical,*, 2016, 237, 373-379.

47. U. Aftab, A. Tahira, A. Gradone, V. Morandi, M.I. Abro, M.M. Baloch, A.L. Bhatti, A. Nafady, A. Vomiero, Z.H. Ibupoto, *Int. j.of hydr. Energy.,* 2021, 46 , 9110-9122.

48. B. M. Abu-Zied, M. M. Alam, A. M. Asiri, J. Ahmed and M. M. Rahman, *Microchemical Journal*, 2020, **157**, 104972.

49. M. M. Rahman, A. Jamal, S. B. Khan and M. Faisal, *The Journal of Physical Chemistry C*, 2011, **115**, 9503-9510.

50. M. M. Rahman, S. B. Khan, M. Faisal, M. A. Rub, A. O. Al-Youbi and A. M. Asiri, *Talanta*, 2012, **99**, 924-931.

51. M. Rahman, S. Khan, G. Gruner, M. Al-Ghamdi, M. Daous and A. M. Asiri, *Electrochimica Acta*, 2013, **103**, 143–150.

52. M. M. Rahman, S. B. Khan, A. M. Asiri, K. A. Alamry, A. A. P. Khan, A. Khan, M. A. Rub and N. Azum, *Microchimica Acta*, 2013, **180**, 675-685.

53. M. M. Hussain, M. M. Rahman, A. M. Asiri and M. R. Awual, *RSC Advances*, 2016, **6**, 80511-80521.

54. Mohammed M. Rahman, M. M. Alam and A. M. Asiri, *RSC Advances*, 2018, **8**, 960-970.

55. A. Wahid, A. M. Asiri and M. M. Rahman, *Environmental Nanotechnology, Monitoring & Management*, 2018, **10**, 314-321.

56. T. A. Sheikh, M. M. Rahman, A. M. Asiri, H. M. Marwani and M. R. Awual, *Journal of Industrial and Engineering Chemistry*, 2018, **66**, 446-455.

57. M. M. Alam, A. M. Asiri, M. T. Uddin, Inamuddin, M. A. Islam, M. R. Awual and M. M. Rahman, *New Journal of Chemistry*, 2019, **43**, 4849-4858.

58. M. M. Alam, A. M. Asiri, M. T. Uddin, M. A. Islam, M. R. Awual and M. M. Rahman, *New Journal of Chemistry*, 2019, **43**, 8651-8659.

59. M. Bhambi, Sum ana G, Malhotra BD, Pundir CS: Artif Cells Blood Substit Immobil Biotechnol, 2010 38, 178-185.

60. S. Roy, N. Soin, R. Bajpai, D. Misra, J.A. McLaughlin, S.S. Roy, *J. of Mater. Chem,* 2011, 21, 14725-14731.

61. S. Amin, A. Tahira, A. R. Solangi, R. Mazzaro, Z. H. Ibupoto, A. Fatima and A. Vomiero, *Electroanalysis*, 2020, **32**, 1052-1059.

62. M. Hussain, Z. H. Ibupoto, M. A. Abbasi, O. Nur and M. Willander, *Journal of Electroanalytical Chemistry*, 2014, **717-718**, 78-82.

63. W. A. Adeosun, A. M. Asiri, H. M. Marwani and M. M. Rahman, *ChemistrySelect*, 2020, **5**, 156-164.

64. M. M. Rahman, J. Ahmed and A. M. Asiri, *RSC Advances*, 2017, **7**, 14649-14659.

65. M. M. Rahman, M. M. Hussain and A. M. Asiri, *New Journal of Chemistry*, 2020, **44**, 19581-19590.

66. X. Chen, J. Zhu, Z. Chen, C. Xu, Y. Wang, C. Yao, *Sens. and Actuat. B: Chemical,* 2011, 159 , 220-228.

67. P.-Y. Kuo, Y.-Y. Chen, *IEEE Trans. Instrum. Meas.* 2021, 70, 1–9.

68. J.-C. Chou, T.-Y. Lai, S.-H. Lin, P.-Y. Kuo, C.-H. Lai, Y.-H. Nien, T.-Y. Su, *IEEE Sens. J.* 2020, 21, 7218–7225.

69. J-C. Chou, T-Y. Lai, Y-H. Nien, C-H. Lai, P-Y. Kuo, S-H. Lin, Y-H. Huang, and K-T. Lee, *Energies*, 2021, 14, 4696

70. S.M. Usman Ali, N.H. Alvi, Z.H. Ibupoto, O. Nur, M. Willander, B. Danielsson, *Sens. Actuators B,* 2011, 152, 241–247.

71. S.M. Usman Ali, Z.H. Ibupoto, C.O. Chey, O. Nur, M. Willander, *Chem. Sens*, 2011, 19, 1–8

72. S.M. Usman Ali, Z.H. Ibupoto, M. Kashif, U. Hashim, M. Willander, *Sensor*s, 2012, 12, 2787-2797

Figure captions

Figure 1: Powder XRD reflections of (a) pristine Co_3O_4 platelets, (b) Co_3O_4 nanowires obtained with cotton silk

Figure 2: Typical SEM images at different magnifications (a, b) pristine Co_3O_4 platelets, (c, d) Co_3O_4 nanowires obtained with cotton silk

Figure 3: EDS spectra (a) pristine Co_3O_4 platelets, (b) Co_3O_4 nanowires

Figure 4: potentiometric response of (a) uricase immobilized pristine Co_3O_4 platelets, (b) , Co_3O_4 nanowires without uricase enzyme immobilization(c)uricase immobilized Co_3O_4 nanowires in various concentrations of uric acid prepared in 0.01M phosphate buffer solution of pH 7.4

Figure 5: Dynamic potentiometric response of uricase immobilized Co_3O_4 nanowires in 1mM uric acid prepared in 0.01M phosphate buffer solution of pH 7.4

Figure 6: Repeatability experiment of uricase immobilized Co_3O_4 nanowires in 0.01M phosphate buffer solution of pH 7.4

Figure 7: Inter electrode response of uricase immobilized Co_3O_4 nanowires in 0.1mM uric acid prepared in 0.01M phosphate buffer solution of pH 7.4

Figure 8: Selectivity response of uricase immobilized Co_3O_4 nanowires in the presence 0.5mM and 0.01mM uric acid and various common interfering substances 0.1mM urea, fructose, ascorbic acid, dopamine, dopamine, and glucose prepared in 0.01M phosphate buffer solution of pH 7.4

Figure 9: (a) effect of various pH values of testing solution on the potentiometric response of uricase immobilized Co_3O_4 nanowires in 0.5mM uric acid prepared in 0.01M phosphate buffer solution, (b) effect of different temperatures on the potentiometric response of uricase immobilized Co_3O_4 nanowires in 0.1 mM uric acid prepared in 0.01M phosphate buffer solution of pH 7.4

Figure 10: EIS simulated Nyquist plots of pristine Co_3O_4 platelets, and Co_3O_4 nanowires with enzyme and without enzyme in 0.1mM uric acid prepared in 0.01M phosphate buffer solution of pH 7.4.

Figure 1

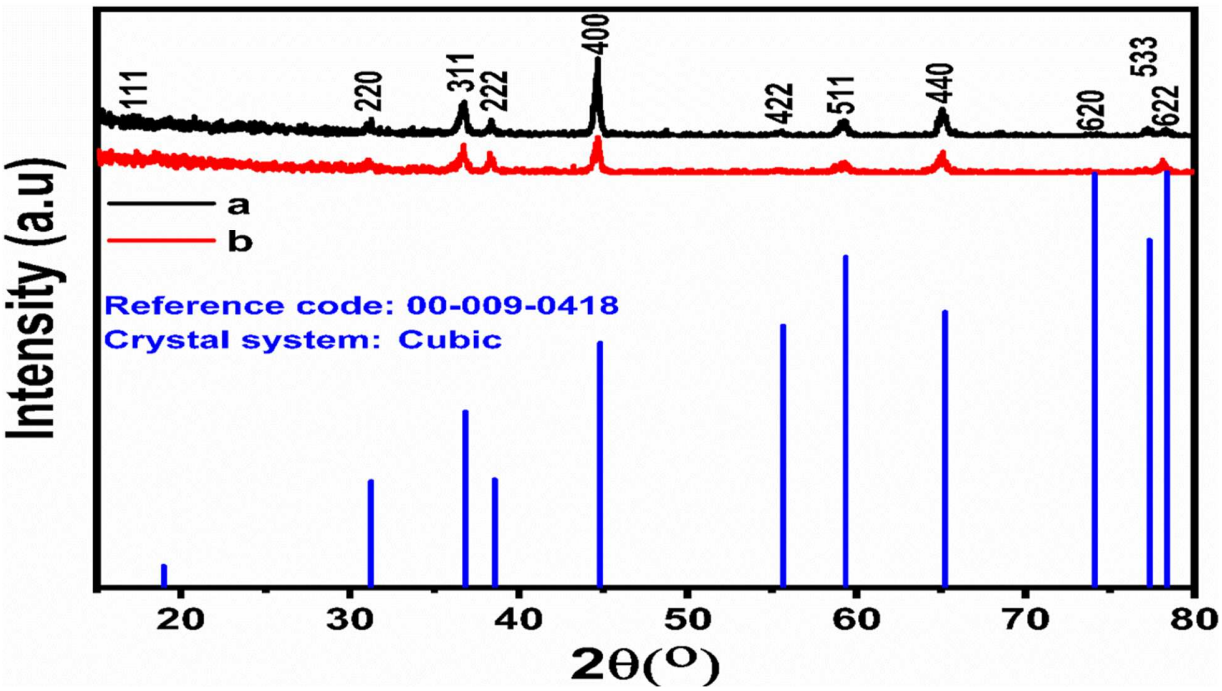
111
220
311
222
400
422
511
440
620
533
622
a
b
Reference code: 00-009-0418
Crystal system: Cubic
Intensity (a.u)
20
30
40
50
60
70
80
2θ(O)

Figure 2

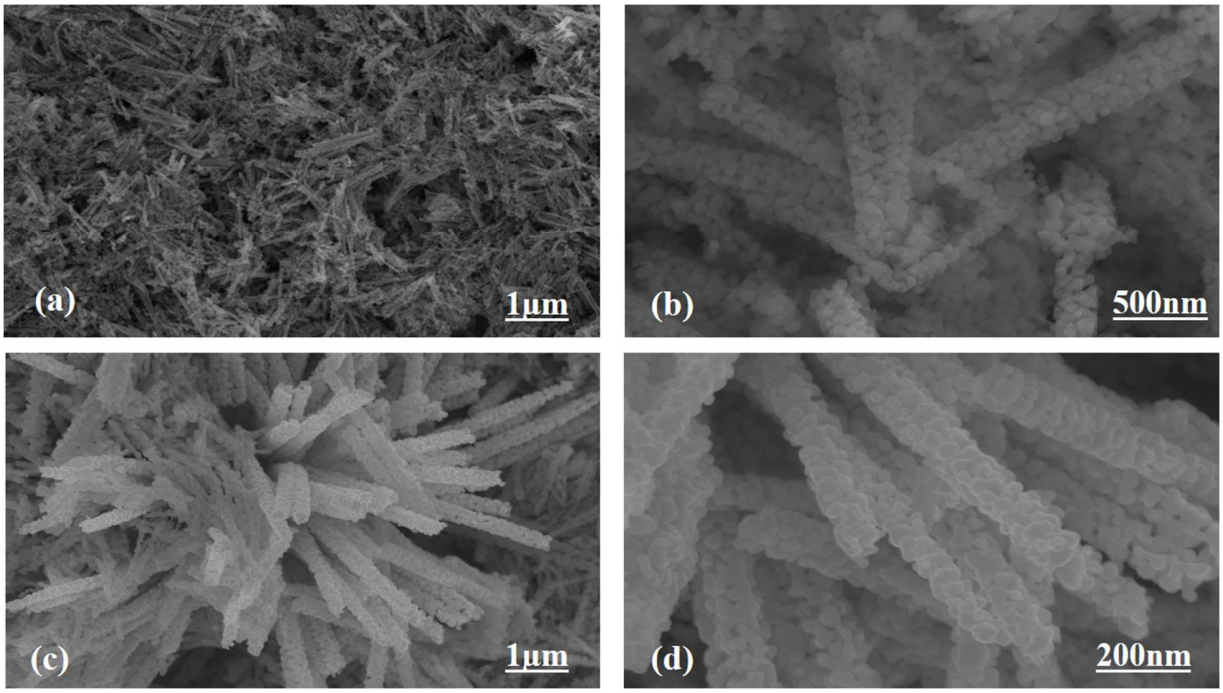

Figure 3

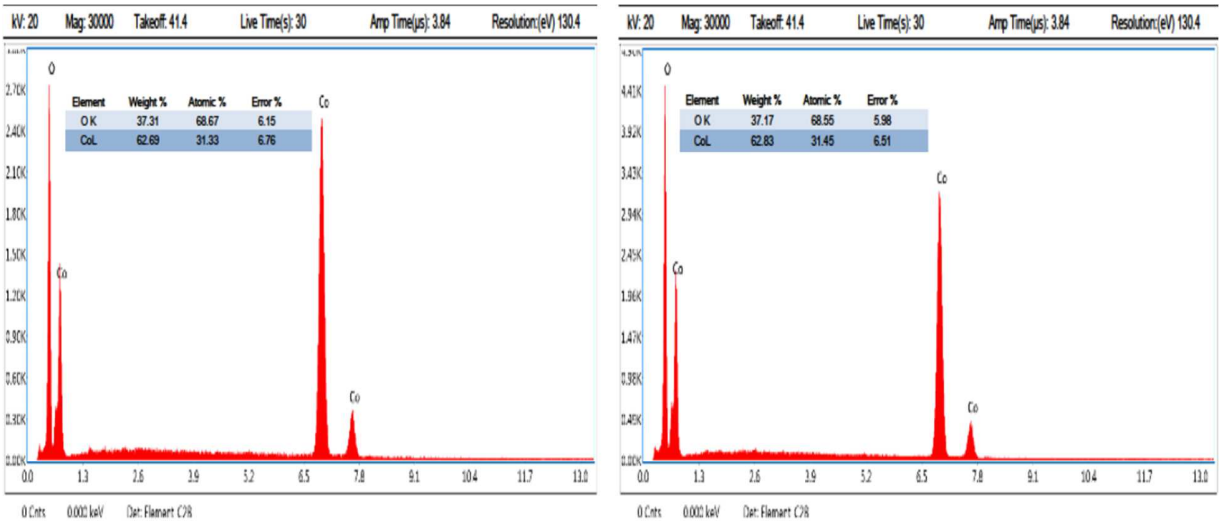
kV: 20 Mag: 30000 Takeoff: 41.4 Live Time(s): 30 Amp Time(us): 3.84 Resolution:(eV) 130.4
O
Co
Co
Co
Element Weight % Atomic % Error %
O K 37.31 68.67 6.15
CoL 62.69 31.33 6.76
0.0 1.3 2.6 3.9 5.2 6.5 7.8 9.1 10.4 11.7 13.0
0 Cnts 0.000 keV Det: Element C28
kV: 20 Mag: 30000 Takeoff: 41.4 Live Time(s): 30 Amp Time(us): 3.84 Resolution:(eV) 130.4
O
Co
Co
Co
Element Weight % Atomic % Error %
O K 37.17 68.55 5.98
CoL 62.83 31.45 6.51
0.0 1.3 2.6 3.9 5.2 6.5 7.8 9.1 10.4 11.7 13.0
0 Cnts 0.000 keV Det: Element C28

(a) **(b)**

Figure 4

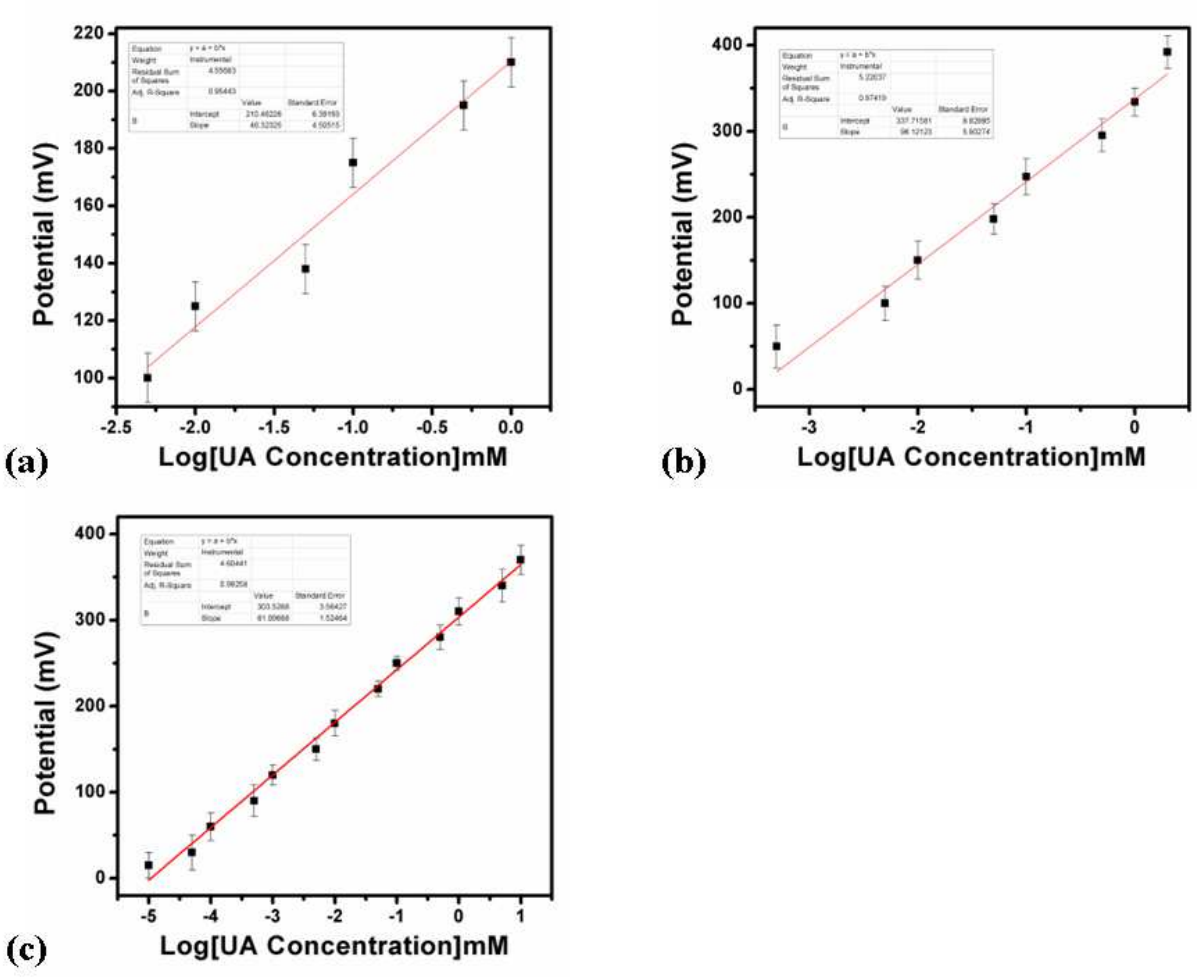

Figure 5

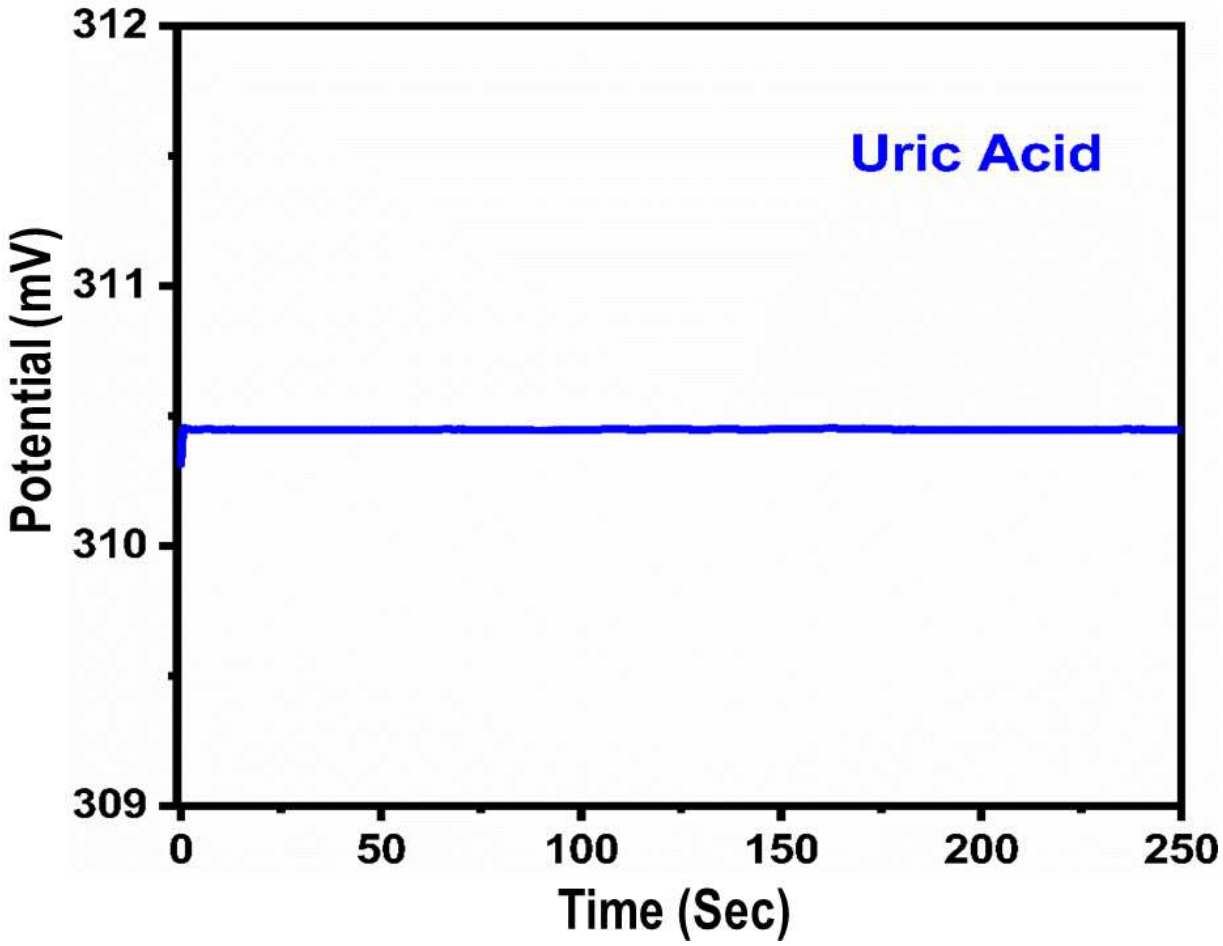
Uric Acid
Potential (mV)
312
311
310
309
0
50
100
150
200
250
Time (Sec)

Figure 6

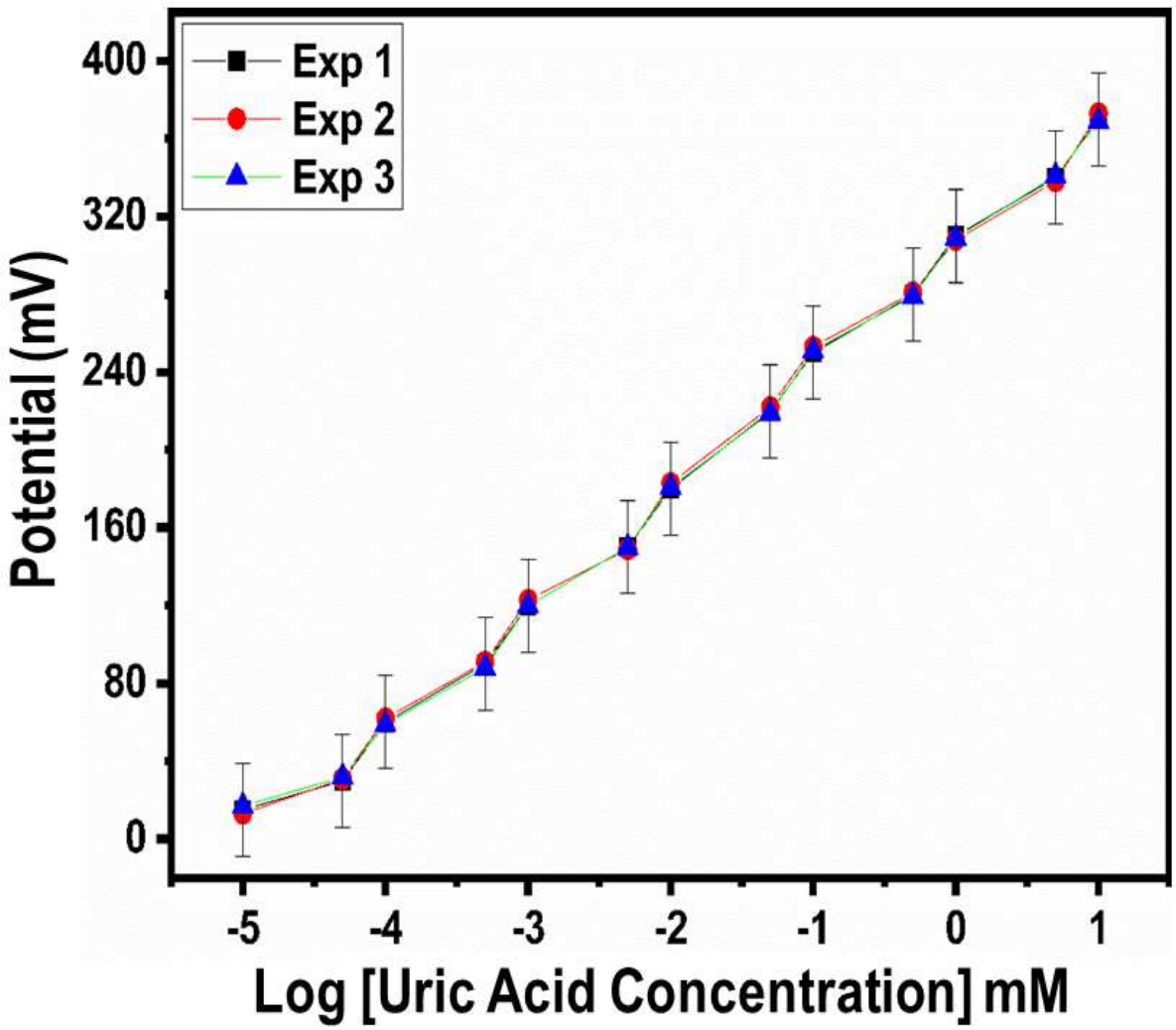
Exp 1
Exp 2
Exp 3
Potential (mV)
400
320
240
160
80
0
-5
-4
-3
-2
-1
0
1
Log [Uric Acid Concentration] mM

Figure 7

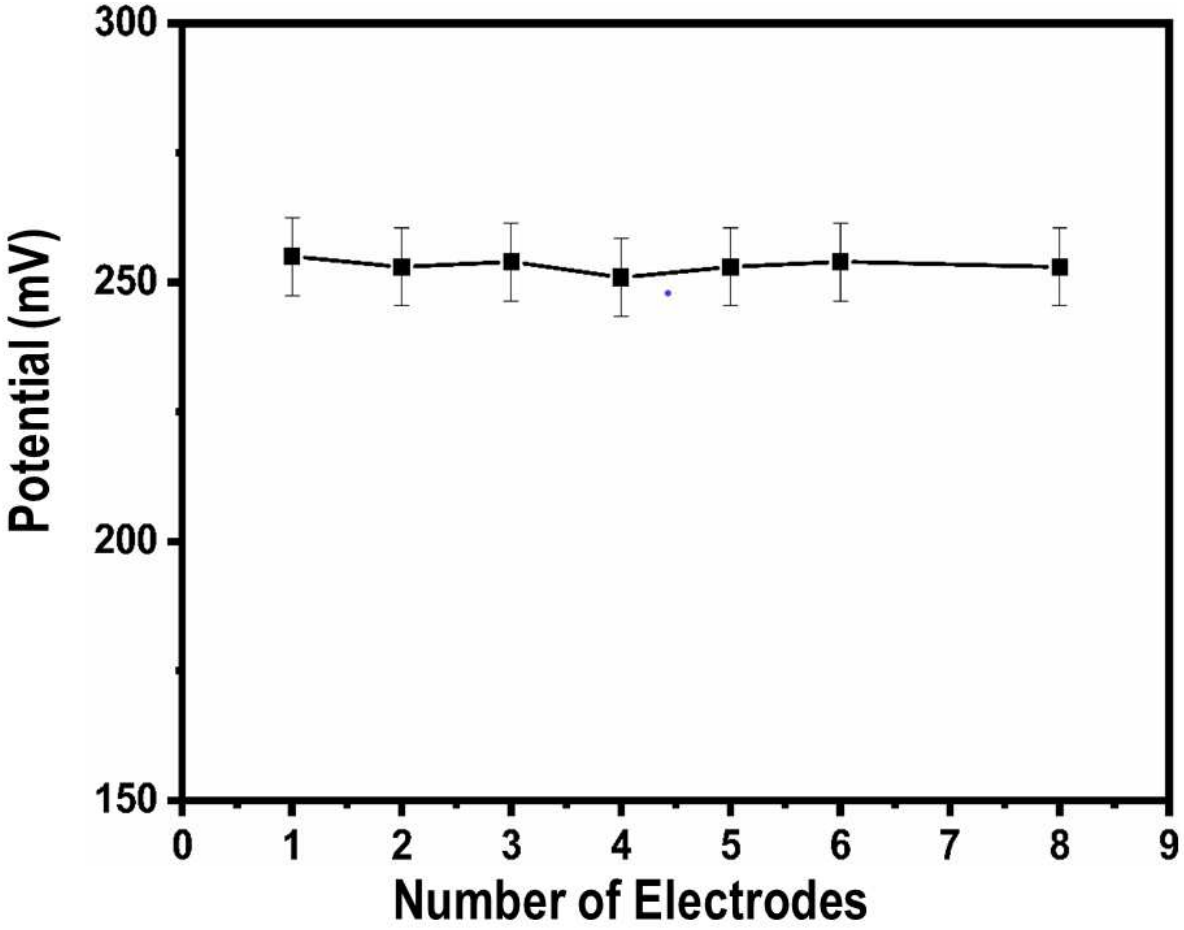
300
250
200
150
Potential (mV)
0
1
2
3
4
5
6
7
8
9
Number of Electrodes

Figure 8

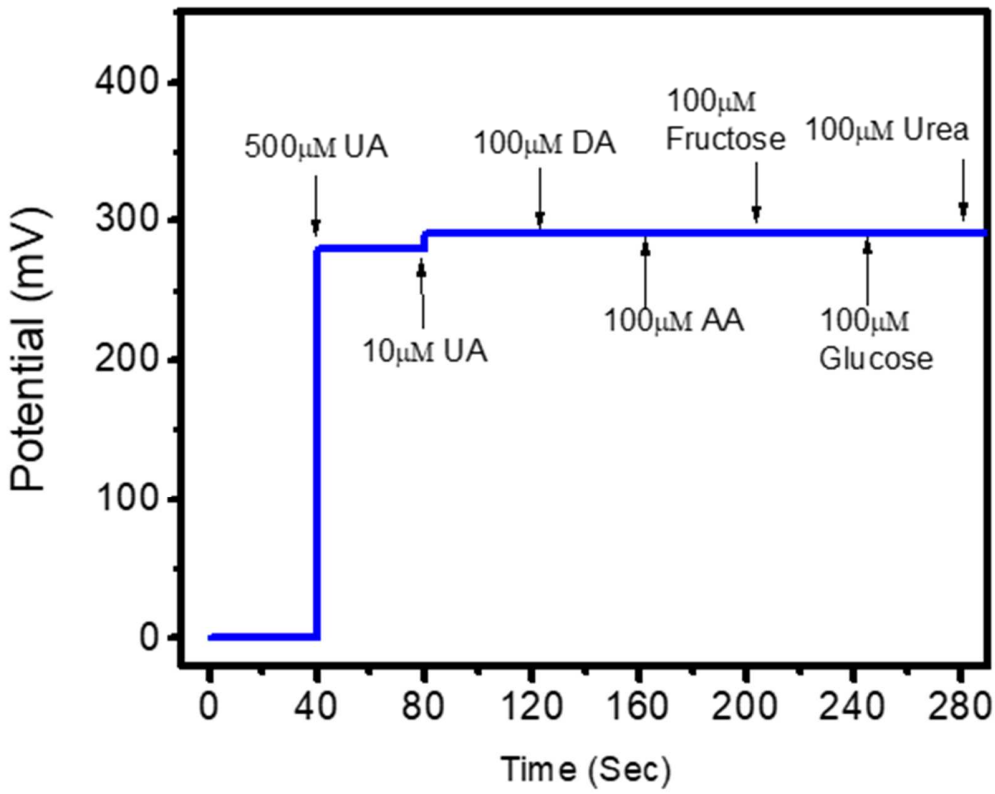
Potential (mV)
400
300
200
100
0
0
40
80
120
160
200
240
280
Time (Sec)
500μM UA
10μM UA
100μM DA
100μM AA
100μM Fructose
100μM Glucose
100μM Urea

Figure 9

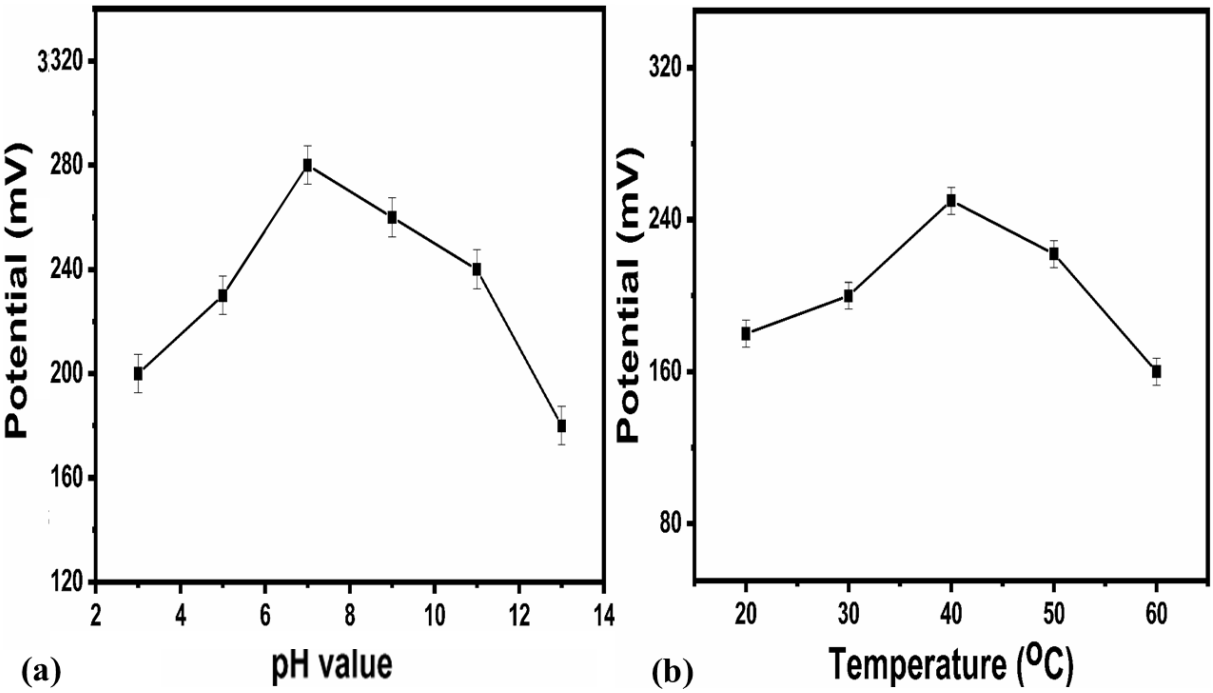
Potential (mV)
3320
280
240
200
160
120
2
4
6
8
10
12
14
pH value
(a)
Potential (mV)
320
240
160
80
20
30
40
50
60
Temperature (°C)
(b)

Figure 10

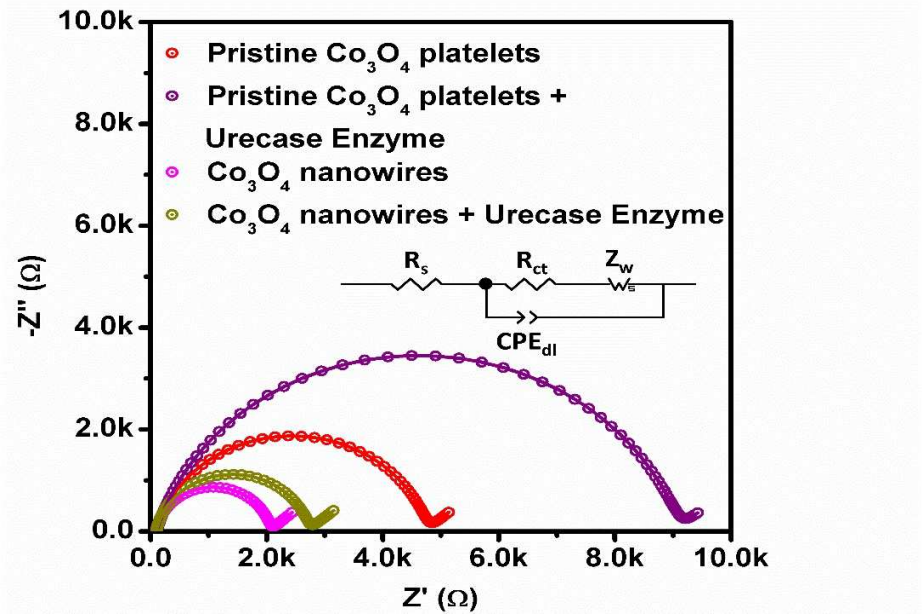

Table 1: Storage period of uricase immobilized Co_3O_4 nanowires

No of weeks	Linear range (mM)	Slope ($mVdec^{-1}$)	Limit of detection (mM)
1	0.0005-10	61.05	0.0001
2	0.0007-10	61.02	0.0003
3	0.0002-10	60.5	0.0004
4	0.0006-9.5	60.8	0.0003
5	0.0003-10	61	0.0001
6	0.0005-10	60.7	0.0002

Table 2: EIS fitted values of charge transfer of Co_3O_4 nanostructures

Materials	**Charge transfer resistance (Ohms)**
Pristine Co_3O_4	4654
Pristine Co_3O_4 +uricase enzyme	8992
Co_3O_4 nanowires	1950
Co_3O_4 nanowires + uricase enzyme	2606

Table 3: % recover of of uricase immobilized Co_3O_4 nanowires

Experiment no:	Added (mM)	Found(mM)	% recovery
1	3	3.1	103.03
2	4	4. 05	101.25
3	5	4.98	99.6

Table 4: Comparative analysis of recently reported potentiometric uric acid biosensors with presented results

Sensing material	**Linear range(mM)**	**Limit of detection (mM)**	**Response time (s)**	**Reference**
RuO_2	0.1-0.5	N/A	N/A	67
MBs–uricase/rGO/NiO	0.1-0.5	0.057	N/A	68
AgNW–uricase/rGO/NiO	0.1-0.5	0.068	N/A	69
ZnO nanowires	0.001-1.0	N/A	6-9	70
ZnO nanotubes	0.005-1.5	N/A	8	71
ZnO nanoflakes	0.0005-1.5	N/A	8	72
Co_3O_4 nanowires	**0.0005-10**	**0.0001**	**1**	**Present work**